Nonlinear Normal Modes of Geometrically Nonlinear Structures using Quasi-static Modal Analysis

Kyusic Park[1] **and Matthew S. Allen**[2]

[1]Graduate Student; UW-Madison - Department of Mechanical Engineering,
[2]Professor; UW-Madison - Department of Engineering Physics
email: kpark93@wisc.edu, matt.allen@wisc.edu

Abstract

Quasi-static modal analysis (QSMA) has begun to gain traction for structures with bolted joints, allowing one to extract the effective modal frequency and damping ratio as a function of amplitude in a fast and accurate manner. This work explores the viability of QSMA to estimate the nonlinear normal modes (NNMs) of geometrically nonlinear structures, where the nonlinearity is much more significant and modal coupling can be far more severe. A quasi-static loading in the shape of a single mode is applied to the nonlinear finite element model in order to retrieve a quasi-static response, using a pseudo-arclength technique, which is capable of continuing through unstable regions for structures undergoing snap through. In the authors' prior works, a secant method was used to estimate the effective natural frequency (i.e. NNM frequency) from the load-displacement curves of the finite element (FE) model. However, that approximation may not be adequate for the strongly nonlinear structures considered in this work. Meanwhile, an alternative method that also utilizes the quasi static response curve is developed; the response curve is fit to a polynomial and used to create a single degree-of-freedom reduced order model (ROM), similar to an implicit condensation (ICE) ROM although the polynomial is allowed to have higher orders than are typically used with ICE. The resulting SDOF ROMs are found to greatly accelerate evaluation of the NNMs while maintaining excellent accuracy. This approach captures the static coupling between the underlying linear modes, but does not capture any additional dynamic coupling. The capabilities of the QSMA approach for estimating NNMs are verified by numerical studies on FE models of various dynamic structures, i.e. a flat clamped-clamped beam, a curved beam and an exhaust cover plate.

Keywords: Nonlinear Dynamics, Quasi-static Modal Analysis, Geometric Nonlinearity, Reduced Order Modeling, Nonlinear Normal Modes

1 Introduction

Nonlinearities in dynamic structures with bolted interfaces have been characterized by the effective natural frequency and nonlinear damping as a function of external load amplitude [1, 2]. Because modeling the bolted joints in a realistic structure is very expensive, yet does not guarantee that its dynamic simulations correlate well with the experiments [3, 4], many advanced methods that simplify joint modeling and analysis were recently introduced [5–7]. Quasi-static modal analysis (QSMA) is one of the approaches for reduced order modeling that assumes the joints behave quasi-statically when they are in a micro-slip regime [8, 9]. In QSMA, one solves for the nonlinear quasi-static response of the structure due to an inertial load, and the resulting modal response is used in conjunction with Masing's rules in order to compute the effective natural frequency and damping ratio of the mode in terms of the load amplitude. The resulting modal model explains how the nonlinear structure would vibrate if each mode was excited separately. A recent work by Lacayo et al. [10] presented a few extensions to the quasi-static method that further simplifies extracting the frequency and damping ratio. Instead of assuming the structure to be nonlinear for lumped bolted joint and linear for the rest of the system, they take the whole system as nonlinear and solve the QSMA problem in one step.

QSMA assumes that the joint structure be can modeled with a superposition of weakly nonlinear modes that are uncoupled when the joints remain in the micro-slip regime. Based on this assumption, the effective natural frequency and damping can be easily estimated from a quasi-static modal response curve of the FE model. Specifically, the secant to the curve can be used to define the modal frequency and the area enclosed by a derived hysteresis curve, i.e. energy dissipated per cycle, can be used to approximate the modal damping ratio. Meanwhile, these modal properties can be related to the nonlinear normal modes (NNMs), which have been acknowledged to be a powerful metric to characterize the oscillation frequency and deformation

shapes of a variety of structures [11]. This work mainly deals with the NNMs of undamped systems although there exist some cases that need to consider the damped NNMs of nonconservative systems [12, 13]. Because NNMs span a range of response amplitudes, are independent of the loading applied to the system and also easily measured from experiments, they have begun to be used to explain the nonlinearity of various dynamic structures [14–17]. Several numerical methods for computing the NNMs of FE models have also been developed such as the pseudo-arclength continuation method in [18], the applied modal force (AMF) method in [19] and the multi-harmonic balance method (MHB) in [20]. Based on the fact that QSMA provides good estimates of the effective natural frequency (i.e. NNM frequency) as well as a significant reduction in the computational cost, this paper explores the viability of the QSMA to estimate the NNMs of dynamic structures that exhibit more complex and stronger nonlinearities compared to the systems with joints that have been studied so far. This paper also focuses on establishing the limits of QSMA, i.e. when and how it breaks down for strongly nonlinear structures.

One way to demonstrate the capability of QSMA in terms of estimating the NNMs of strongly nonlinear structures is to apply the approach to a structure with a geometric nonlinearity, which typically becomes important when the structure shows large deformations. Snap-through buckling of wing panels [21, 22] and unstable fluttering of curved plates [23] are good examples of structures exhibiting nonlinearities due to large deformations. The NNMs of these models have recently been used for model updating and to compare different nonlinear models [24–27]. For instance, the NNM backbone curves of flat beam models were iteratively computed and compared with experimental data to optimize model parameters by using the nonlinear least squares approach in [24], and the Bayesian approach in [26]. However, directly computing the NNMs of a FE model can be prohibitively expensive, especially if many elements are needed to describe the geometry. Moreover, while the computation cost may be feasible for small to moderately sized FE models, it can still be demanding, especially if the structure has many internal resonances so that the NNMs become intricate to compute; such is often the case for complicated structures. To circumvent the computational issue, many reduced order modeling frameworks have been devised that significantly reduce the degrees of freedom but accurately capture the NNMs of a nonlinear FE model. Largely there are two approaches to generate a reduced order model (ROM), i.e. direct methods and indirect methods [28, 29]. Direct methods are not considered in this paper as they naively require the full order nonlinear stiffness matrices in order to perform the DOF reduction, and most commercial FE packages do not give the user access to the required information. On the other hand, indirect methods such as the enforced displacement (ED) method and the implicit condensation and expansion (ICE) method use a set of static displacement (or load) cases in the shape of few dominant modes in order to project the nonlinear response onto the reduced set of modal basis. In a recent work of Kuether et al. [30], the ED and ICE methods were demonstrated on FE models of geometrically nonlinear structures, such as an exhaust cover plate, and showed that the resulting multi-mode ROMs were capable of reproducing the backbone curves of the full FE model accurately. This also implies that the NNM will match the dynamic response in a variety of loading conditions and over a range of loading amplitudes, and hence is a useful metric for evaluating ROMs.

Despite the advantages of indirect methods, their accuracy is sensitive to a load scaling factor that is used to set the amplitude of the static displacements (or loads) that are applied. Furthermore, they typically include multiple modes and so one cannot filter out the internal resonance branches. This is problematic if one wishes to use a ROM when updating a FE model to correlate with measurements; the backbones are of primary interest in that application and yet they become difficult to compute as the algorithm can get stuck trying to resolve the internal resonances. On the other hand, QSMA only requires a modal load-displacement curve for computing the NNMs and it inherently filters out the internal resonance branches. Thus, it is meaningful to investigate the possibility of using QSMA to estimate the NNMs of geometrically nonlinear structures. The numerical results presented in this paper show that QSMA can be advantageous in some cases to provide a good initial guess of NNMs, even when one's primary goal is to study strongly nonlinear systems. Nevertheless, the limits of QSMA in terms of accuracy, in cases where the nonlinearity is quite large, is investigated. Meanwhile, an alternative method for using the QSMA load-displacement curves to compute the NNMs is presented, which significantly improves the accuracy of the backbone curves. The proposed method generates a single degree of freedom (SDOF) ROM whose nonlinear stiffness terms can be identified by a least-squares fitting to the modal response curve. Due to the similarity to the ICE method, the resulting model can be regarded as a SDOF ICE ROM. The compactness and accuracy of the alternative method are investigated in detail to demonstrate that the resulting ROM consists of nonlinear stiffness terms whose order is greater than cubic in order to implicitly account for the static modal coupling between the underlying linear modes. A very recent work of Hill et al. [31] also showed that a SDOF ICE ROM needs to consist of nonlinear terms greater than cubic to accurately capture the static effects of the underlying linear modes. The comparison between the secant method and the SDOF ICE method reveals that the original QSMA can be extended to create a mix between the QSMA and the ICE, which highlights the limits of the secant method and shows the importance of higher-order polynomial terms in ICE.

This paper is organized as follows. Section 2 outlines definitions of a geometrically nonlinear FE model and its quasi-static modal response followed by derivations of two methods (i.e. the secant method and the SDOF ICE method) for computing NNMs. In Section 3, the proposed methods are demonstrated on three numerical examples, i.e. a flat clamped-clamped beam, a curved beam and an exhaust cover plate, in order to explore their characteristics and accuracies in terms of estimating NNMs

of geometrically nonlinear structures. The conclusions and some aspects of future work are presented in Section 4.

2 Theory

2.1 Geometrically Nonlinear Finite Element Model

The n-DOF FE model that exhibits geometric nonlinearity can be expressed as

$$\mathbf{M}\ddot{\mathbf{x}} + \mathbf{C}\dot{\mathbf{x}} + \mathbf{K}\mathbf{x} + \mathbf{f}_{\text{nl}}(\mathbf{x}) = \mathbf{f}(t) \tag{1}$$

where $\mathbf{M}, \mathbf{C}$ and $\mathbf{K}$ are the n x n mass, damping and stiffness matrices and $\mathbf{f}(t)$ is the n x 1 external force. The n x 1 nonlinear restoring force $\mathbf{f}_{\text{nl}}$ captures the geometric nonlinearity of the model, which is a function of the displacement vector $\mathbf{x}$. The full equations of motion of the FE model can be transformed from a physical space to a modal subspace by solving an eigenvalue problem:

$$(\mathbf{K} - \omega_r^2\mathbf{M})\mathbf{\Phi}_r = 0 \tag{2}$$

where ω_r is the r-th linear natural frequency and $\mathbf{\Phi}_r$ is its n x 1 mode shape. Then, the FE model can be approximated with a superposition of a subset of the linear modes as

$$\mathbf{x} = \mathbf{\Phi}_m\mathbf{q} \tag{3}$$

where $\mathbf{q}$ is the m x 1 modal displacement and $\mathbf{\Phi}_m$ is the n x m mass normalized mode shape matrix. The reduced DOF of modal coordinates can be significantly smaller than the DOF of original physical coordinates ($m \ll n$). Then, the r-th nonlinear modal equation can be written as

$$\ddot{q}_r + c_r\dot{q}_r + \omega_r^2 q_r + \theta_r(q_1, q_2, ..., q_m) = \mathbf{\Phi}_r^T\mathbf{f}(t) \tag{4}$$

where the nonlinear restoring force θ_r is a function of the modal displacements $\mathbf{q}$. It was shown in recent works (e.g. [28, 30]) that the nonlinear restoring force that captures only the geometric nonlinearity of a linear elastic system are well approximated with a 3rd order polynomial as

$$\theta_r(q_1, q_2, ...q_m) = \sum_{i=1}^{m}\sum_{j=i}^{m} A_r(i,j)q_i q_j + \sum_{i=1}^{m}\sum_{j=i}^{m}\sum_{k=j}^{m} B_r(i,j,k)q_i q_j q_k \tag{5}$$

where A_r and B_r are the quadratic and cubic nonlinear stiffness terms, respectively. The ICE method in [30] applies a set of static loads, which consists of a linear combination of multiple mode shapes, to the FE model in order to find nonlinear stiffness terms. The ICE ROM also typically uses up to cubic order polynomial, and incorporates multi modes to accurately capture the coupling between the reduced modal basis.

2.2 Quasi-static Modal Response

The QSMA method assumes that the FE model would deform by the quasi-static force in the same way that it would deform dynamically if it were vibrating in only the mode in question. The external force defined by the r-th linear mode shape, which is proportional to $\mathbf{M}\mathbf{\Phi}_r$, will dominantly excite the r-th linear mode of the FE model because the orthogonality of linear modes is still valid in the weakly nonlinear regime. The quasi-static problem with respect to the r-th modal force can be expressed as

$$\mathbf{K}\mathbf{x} + \mathbf{f}_{\text{nl}}(\mathbf{x}) = \mathbf{M}\mathbf{\Phi}_r\alpha \tag{6}$$

where α is the modal force amplitude. Then, the r-th quasi-static modal response $q_r(\alpha)$ can be mapped from the physical quasi-static response $\mathbf{x}(\alpha)$ of Eqn. 6

$$q_r(\alpha) = \mathbf{\Phi}_r^T\mathbf{M}\mathbf{x}(\alpha) \tag{7}$$

It can be interpreted that the internal force that is at equilibrium to the quasi-static loading is captured and projected onto the r-th mode. By pre-multiplying Eqn. 6 by $\mathbf{\Phi}_r^T$, the r-th modal force-response can be explained in terms of α and q_r in the modal subspace by the following equation

$$\omega_r^2 q_r + \theta_r(q_r) = \alpha \tag{8}$$

where $\theta_r(q_r)$ is the modal nonlinear restoring force defined by the single modal coordinate q_r. Note that the quasi-static modal response implicitly captures the static effects of other linear modes, i.e. $\theta_r(q_r) = \mathbf{\Phi}_r^T\mathbf{f}_{\text{nl}}(\mathbf{x}) = \mathbf{\Phi}_r^T\mathbf{f}_{\text{nl}}(\mathbf{\Phi}_m\mathbf{q})$. The unknown nonlinear function $\theta_r(q_r)$ can be derived by using Riks method and least-squares fitting, as explained in the following section.

2.3 Quasi-static Response Curve Fitting

In this work, the quasi-static response in Eqn. 6 can be found using Riks method. Riks method is a powerful tool that captures the geometric instabilities such as snap through behavior when computing load-displacement curves. The implementation of Riks method that was used in this work is based on a pseudo-arclength continuation technique, which was presented in detail in [32]. The resulting quasi-static response $\mathbf{x}(\alpha)$ can be converted to the quasi-static modal response $q_r(\alpha)$ by Eqn. 7. Then, the load α_j and response $q_r(\alpha_j)$ are known at ns samples (load amplitudes), and this data can be used to find the nonlinear function $\theta_r(q_r)$. The unknown function $\theta_r(q_r)$ is approximated by a polynomial, i.e. $\theta_r(q_r) = \sum_{i=2}^{l} k_i q_r^i$ where k_i is the i-th nonlinear stiffness coefficient and l is the highest order of the nonlinear terms. Hence, one must simply estimate k_is from the load-displacement data, by minimizing the least-squares cost function J that is defined as follows.

$$\min_{\{k_2,k_3,\ldots,k_l\}} J = \sum_{j}^{ns} \frac{\left(w_r^2 q_{r,j} + \theta_r(q_{r,j}) - \alpha_j\right)^2}{\alpha_j^2} = \sum_{j}^{ns} \frac{\left(w_r^2 q_{r,j} + \sum_{i=2}^{l} k_i q_{r,j}^i - \alpha_j\right)^2}{\alpha_j^2} \tag{9}$$

By completing all the above processes, the undamped and unforced SDOF equation of motion in r-th mode, can be formulated as

$$\ddot{q_r} + \omega_r^2 q_r + \sum_{i=2}^{l} k_i q_r^i = 0 \tag{10}$$

Compared to the ICE method, the QSMA approach only uses a single mode, but higher order nonlinear terms greater than cubic, in order to capture the static effects of modes that are not included in the modal basis. In fact, Hill et al. [31] recently showed that a single DOF ICE ROM needs to consist of nonlinear terms greater than 3rd order (cubic) to accurately capture the static effects of the modes that have been neglected when reducing the basis (i.e. statically reducing those modes out of the modal basis). Also, note that the QSMA approach fully utilizes a continuous set of data from the quasi-static response curve in order to find the nonlinear terms, whereas ICE typically uses a minimal set of load data, i.e. loading at $-\alpha_r$ and $+\alpha_r$ for each mode and for each combination of modes. Thus, the equation obtained by the QSMA approach (Eqn. 10) can be regarded as a SDOF ICE ROM that uses higher order nonlinear stiffness terms. In the following, these QSMA derived ROMs will be called SICE ROMs.

2.4 NNM Evaluation based on QSMA Approach

QSMA has previously only been used to estimate the amplitude-dependent frequencies of the structures with nonlinear joints. In all applications to date, the slope of a secant line of the quasi-static modal response $q_r(\alpha)$ was used to define the natural frequencies ω_r of the system at each load amplitude α as follows.

$$\omega_r(\alpha_j) \triangleq \sqrt{\frac{\alpha_j}{q_r(\alpha_j)}} \tag{11}$$

In prior works, where the structures all exhibited weak nonlinearities due to the bolted joints, the secant approximation from the QSMA has provided an accurate estimate of the natural frequencies [10]. However, the geometrically nonlinear structures considered here contain much stronger nonlinearities, and so the secant approximation may be accurate only for small frequency shifts.

In order to accurately capture the geometric nonlinearities over a larger frequency range, the SICE ROM in Eqn. 10 can be utilized. In other words, the SICE ROM can be used to compute the NNMs of the nonlinear structure. In this paper, the NNM computation is performed by a shooting and pseudo-arclength continuation method, which was presented in [18]. Meanwhile, the NNMs of the original FE models were also computed by the applied modal force (AMF) method in [19] and the multi harmonic balance (MHB) method in [20], which serve as reference curves against which the curves obtained here by QSMA with the secant and SICE methods can be compared to evaluate their accuracy.

3 Numerical Studies

In this paper, three numerical studies are illustrated to show the effectiveness of the QSMA approach for computing NNMs of the geometrically nonlinear structures. The first study evaluates the NMMs of a flat clamped-clamped beam that exhibits relatively weak nonlinearity. The second example is an exhaust cover plate that is more realistic and exhibits some internal modal coupling. We lastly examine a curved beam that experiences not only strong modal interaction but also dynamically

unstable snap-through. All of the required routines including the quasi-static response computation and the NNM computation were implemented in MATLAB®.

3.1 Flat Clamped-Clamped Beam

This geometrically simple beam exhibits hardening nonlinearities at large transverse displacements, and has been used in several previous works to study these phenomena [30, 33, 34]. The beam FE model used here has the same geometry and material properties as the beam studied in [30]. The dimensions of the beam are as follows: 228.6 mm in length, 12.7 mm in width and 0.787 mm in thickness. The beam was meshed with 40 2-node beam elements that resulted in 117 free DOF. The material properties of the model are based on steel with a Young's modulus of 204.8 GPa, a Poisson's ratio 0.29 and a mass density 7870 kg/m^3. The r-th linear normal mode $\mathbf{\Phi}_r$ and its natural frequency ω_r were then computed by Eqn. 2. The geometry of the flat beam and its first four bending modes are shown in Figure 1.

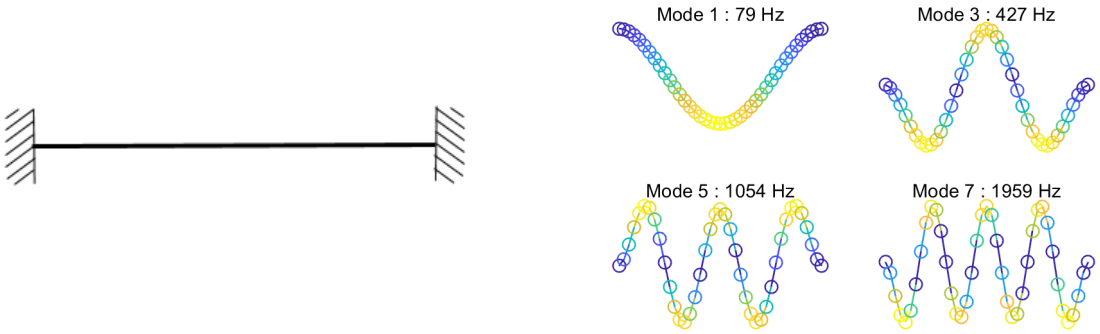

Figure 1: The flat clamped-clamped beam model and its dominant modes.

3.1.1 Quasi-static Response Curve

The nonlinear quasi-static response of the beam model was then found when a force given by Eqn. 6 was applied to the structure. The response of the full FE model was found, yet in Figure 2 we only plot the response of the center node, x_c, versus load amplitude. The hardening behavior of the beam, that is due to the coupling between the bending and membrane motions, can be seen in the load displacement curve. The maximum displacement of the center node ($x_{c,\max}$ = 2.7788 mm) was set to be about 350% of the beam thickness such that the nonlinearity of the beam could be sufficiently captured for large deflection.

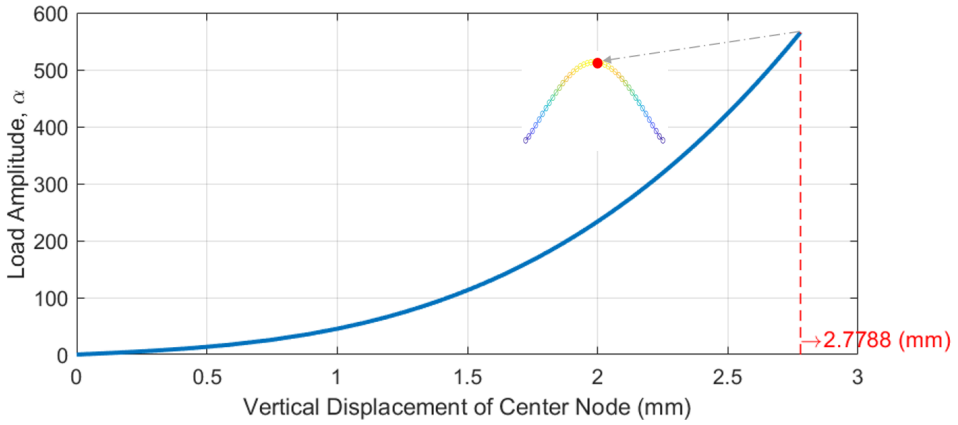

Figure 2: The quasi-static response of the flat clamped-clamped beam for Mode 1. The curve traces the center node displacement of the beam model with respect to the load scaling factor α.

The peak modal displacements $q_{r,c}$ of the first five dominant bending modes, that were mapped from the physical displacement by Eqn. 7, are shown in Figure 3. It can be inferred from the modal response curves that the bending mode 3 is the most strongly coupled mode with respect to the first bending mode. The maximum amplitude of Mode 3 ($q_{3,c,\text{max}} = 0.1935$ mm) was about 6% of that of the first mode ($q_{1,c,\text{max}} = 2.9335$ mm) when the center node reached the maximum displacement.

The nonlinear stiffness coefficients of various SICE ROMs were identified by least-squares fitting to the target modal response curve for the first mode. The data consisted of 84 data samples ($ns = 84$). The fitted curves of the SICE ROMs of different orders are shown in Figure 3. The fitting errors in Eqn.9 are also presented in Table 1, which show only 0.033% error when the 4th order polynomial is used ($l = 4$) for the flat clamped-clamped beam model. The resulting coefficients can be found in Table 2.

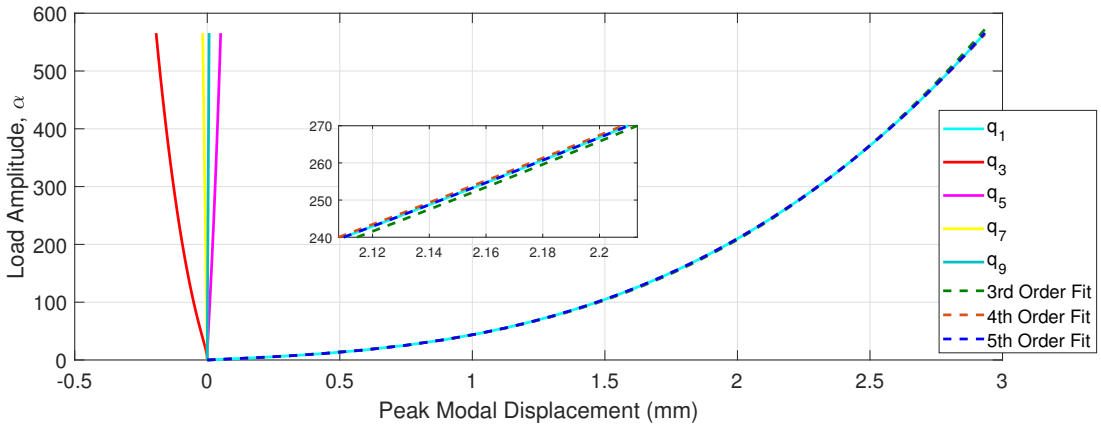

(a)

Figure 3: The quasi-static response of the first five dominant bending modes of the flat clamped-clamped beam model. The dashed curves illustrate the least-squares fitted curves of a 3rd order, a 4th order and a 5th order SICE ROM to the first modal response curve.

Fitting order (l)	3	4	5
Fitting error (J)	0.00674	0.00033	3.50e-06

Table 1: The least-squares fit error J in Eqn. 9 to the first modal response curve of the flat clamped-clamped beam model.

Order	1st	2nd	3rd	4th
Coefficient (k_i)	2.4619e+5	1.1532e+9	3.8030e+13	-2.1887e+16

Table 2: The coefficients of the 4th order SICE ROM (SICE-4) of the flat clamped-clamped beam.

Note that the comparison so far only demonstrates how accurate the SICE ROM can capture the static response. In order to evaluate how well the dynamic responses are captured by this ROM as well as when using the conventional secant method, the NNMs are computed and compared in the next section.

3.1.2 NNM Evaluation

The first NNM of the flat beam was computed using the secant method in Eqn. 11 and the SICE ROMs with the shooting and pseudo-arclength continuation method in [18]. In order to have an estimate of the "true" NNM against which to compare these, the first NNM curve of the full FE model was also computed by the AMF algorithm in [19]. Figure 4 illustrates the resulting curves of each method in the frequency-modal response plane. Note that the extent of quasi-static modal response (0 mm $\leq q_{1,c} \leq 2.9335$ mm), which was used to generate the SICE ROMs, sufficiently covers that of dynamic responses considered in the NNM computation (0 mm $\leq q_{1,c}^{\text{nnm}} \leq 1.9515$ mm). Otherwise, the resulting SICE ROMs could not fully capture the nonlinearties in the dynamic responses.

The secant method approximates the natural frequencies of the beam model well for small deformations ($q_{1,c} \lessapprox 0.1$ mm). However, as the deformation further increases, its NNM curve deviates from the backbone curve of the full FE model. On the other hand, the first NNM curve computed with a 4th order SICE ROM (SICE-4) accurately matches with the reference curve. This indicates that the hardening nonlinearity of the flat beam structure can be well captured by a 4th order SDOF equation. Hence, as the beam vibrates in this mode, the other modes are important only in their contribution to the effective stiffness of this mode - they are statically condensed into q_1. It is also noticeable that the third order SICE ROM (SICE-3) produces relatively larger errors in the NNM even though it had small error in terms of the least-squares fitting to the quasi-static modal response curve.

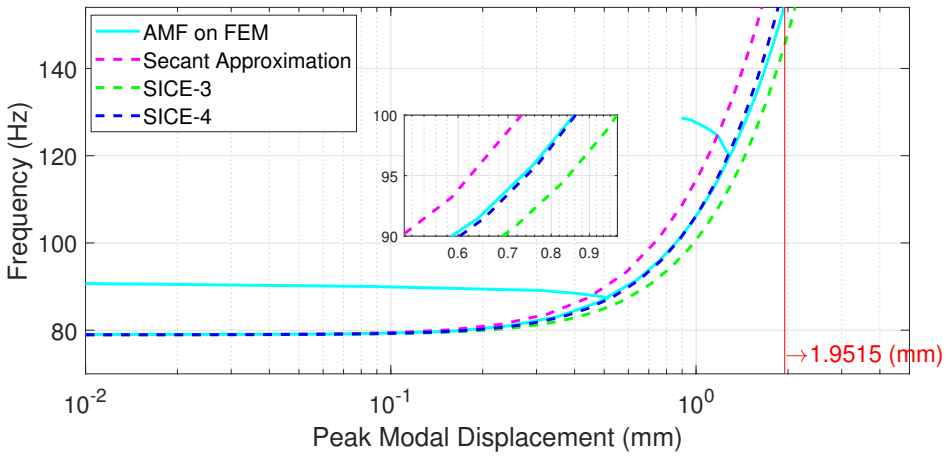

(a)

Figure 4: The first NNM curves of the flat clamped-clamped beam in the frequency-modal response plane: the NNM curve computed by the secant method and the NNM curves computed with a 3rd order SICE ROM (SICE-3) and a 4th order SICE-ROM (SICE-4).

3.2 Exhaust Cover Plate

QSMA approach was also applied to estimate the NNMs of a FE model of an exhaust cover plate, whose geometric nonlinearities were investigated in a few recent works [19, 30, 35]. They discovered a significant coupling between the first and sixth modes. The geometry and material properties of our FE model follow those of the plate model in [30]. The provided dimensions and properties are as follows: 317.5 mm in diameter, 208 GPa for a Young's modulus, 0.3 for a Poisson's ratio, 7800 $\mathrm{kg/m^3}$ for a mass density such that the model approximates a thin circular steel plate. The plate was composed of 1440 4-node shell elements of 1.5 mm thickness that resulted in 8406 free DOF. The nodes at the very bottom are fixed approximating the boundary as infinitely stiff. The FE plate model and some of its linear bending modes are shown in Figure 5.

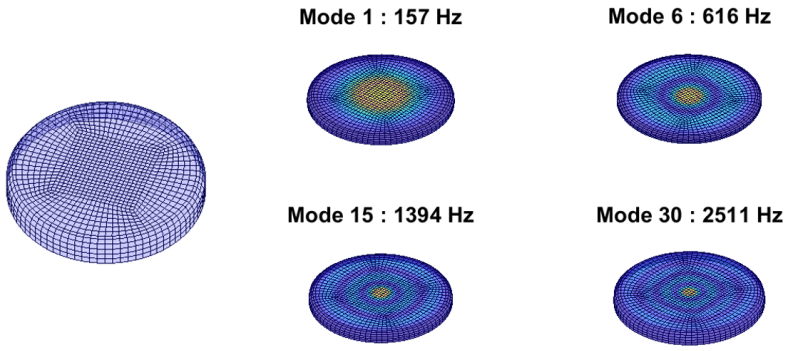

Figure 5: The finite element model of the exhaust cover plate and its dominant modes.

3.2.1 Quasi-static Response Curve

The nonlinear quasi-static response of the plate model subject to the first linear modal force ($\mathbf{f} = \mathbf{M}\mathbf{\Phi}_1\alpha$) is presented in Figure 6. Similar to the flat clamped-clamped beam model, hardening behavior can be observed at large transverse displacements. The maximum vertical displacement of the center node $x_{c,\max}$ was set to be about 300% of the thickness of the plate model. Figure 7 demonstrates the quasi-static modal response curves $q_{r,c}$ of four dominant bending modes. The maximum peak modal displacement of Mode 6 ($q_{6,c,\max} = 0.8450$ mm) was about 15% of that of the first mode ($q_{1,c,\max} = 5.5695$ mm), which indicates 1) a strong modal coupling between the first and the sixth mode and 2) that the plate model has relatively stronger modal coupling compared to the flat beam model.

The least-squares fitted curves of various SICE ROMs of the first mode are also shown in Figure 7. The fitting errors in Table 3 were computed when 119 samples ($ns = 119$) were used for the fitting. The mean fitting error, i.e. $J_{\text{avg}} = \frac{J}{ns}$, of the SICE-3 of the exhaust cover plate was almost twice as much as that of the SICE-3 of the flat clamped-clamped beam. On the other hand, the SICE-4 showed a similar mean error to that of the SICE-4 of the beam model, whose coefficients are presented in Table 4.

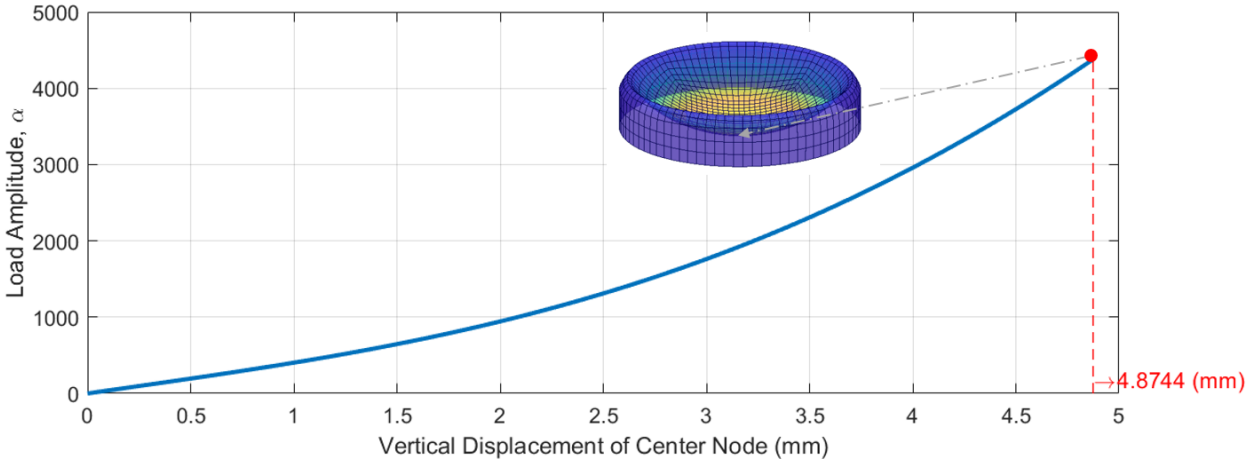

Figure 6: The quasi-static response of the exhaust cover plate for Mode 1. The curve traces the displacement of the center node of the plate model, with respect to the load scaling factor α.

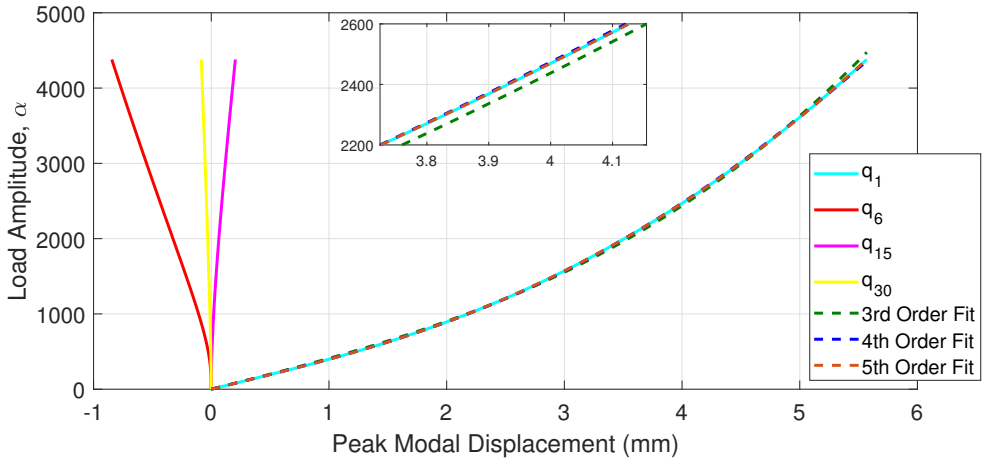

(a)

Figure 7: The quasi-static response of the first four dominant bending modes of the exhaust cover plate model. The dashed curves illustrate the least-squares fitted curves of a 3rd order, a 4th order and a 5th order SICE ROM to the first modal response curve.

Fitting order (l)	3	4	5
Fitting error (J)	0.01840	0.00059	4.00e-06

Table 3: The least-squares fit error J in Eqn. 9 to the first modal response curve of the exhaust cover plate model.

Order	1st	2nd	3rd	4th
Coefficient (k_i)	9.7333e+5	-1.0918e+8	3.8782e+11	-6.6320e+13

Table 4: The coefficients of the 4th order SICE ROM (SICE-4) of the exhaust cover plate.

3.2.2 NNM Evaluation

The first NNM of the exhaust cover plate was computed using the secant method and the SICE method and both curves are shown in Figure 8. The NNM curves are compared with a reference NNM curve of the full FE model, that was computed by the AMF method. The secant method starts to induce errors when the deformation reaches about 2% of the plate thickness ($q_{1,c} \approx 0.1$ mm) and shows a spurious softening nonlinearity that is not present in the AMF solution. On the other hand, the backbone curve of the SICE-4 accurately matches with that of the full FE model, indicating that the plate's hardening behavior can be accurately simulated by a 4th order SDOF polynomial. This 4th order SICE model only contains the static modal coupling shown in Figure 7, and so this reveals that the first NNM of this structure can be captured accurately if one captures the static modal coupling; this mode doesn't exhibit any additional dynamic modal coupling that is important.

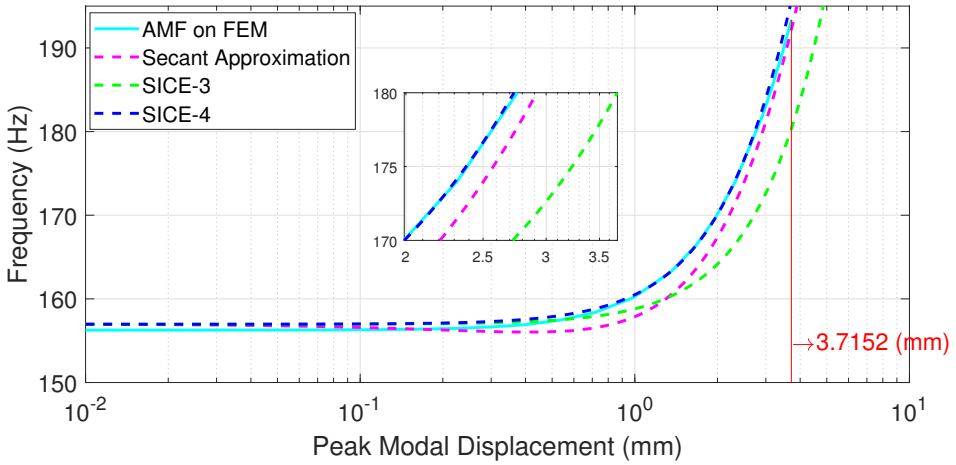

(a)

Figure 8: The first NNM curves of the exhaust cover plate in the frequency-modal response plane: the NNM curve computed by the secant method and the NNM curves computed with a 3rd order SICE ROM (SICE-3) and a 4th order SICE-ROM (SICE-4).

3.3 Curved Beam

The curved beam exhibits a snap-through behavior as well as strong interactions between low and high frequency modes, that were previously studied in [27, 36, 37]. This numerical study investigates the capability of the QSMA approach with respect to such a highly unstable and nonlinear structure. The geometry and material properties of the FE model of the curved beam are the same as those of the shallow curved beam model in [37]. The length, l is 304.8 mm, width is 12.7 mm and thickness is 0.508 mm. The radius of curvature, R is defined to be 11430 mm so that the maximum rise is twice the thickness of the beam (h = 1.016 mm). The Young's modulus is 206.84 GPa, Poisson's ratio is 0.29 and mass density is 7800 kg/m^3, again approximating steel. The beam model is meshed with a hundred 2-node beam elements to have 297 free DOF. The FE model of the curved beam and its dominant bending modes are depicted in Figure 9.

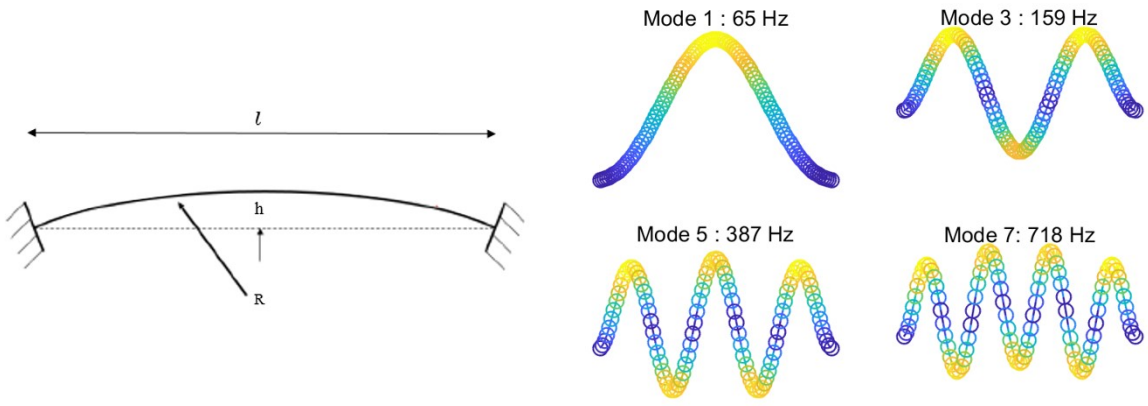

Figure 9: The finite element model of the curved beam and its dominant modes.

3.3.1 Quasi-static Response Curve

The nonlinear quasi-static response of the curved beam FE model with respect to the first linear modal force is displayed in Figure 10. A softening followed by hardening behavior appears when the vertical deflection is from one to four times the beam thickness, as can be seen in the zoomed-in plot. The maximum value of the center node displacement was set to be about ten times the beam thickness to fully capture the hardening nonlinearity at large deformations. Figure 11 illustrates the quasi-static response curves of the dominant bending modes, and it can be seen that Mode 3 is strongly coupled with the first mode, i.e. the maximum amplitude of the Mode 3 ($q_{3,c,\max} = 0.8837$ mm) was about 14% of that of the first mode ($q_{1,c,\max} = 6.2150$ mm) when the center node displacement was at the maximum.

The least-squares fitted curves of the SICE ROMs are also illustrated in Figure 11. For the fitting, 149 sample points ($ns = 149$) were used and the resulting errors are presented in Table 5. The nonlinear quasi-static modal response of the curved beam was not well approximated by low order SICE ROMs such as SICE-3 or SICE-4. The fitting accuracy was enhanced for the SICE-5, yet there was still some error in the snap-through response. When the order was increased to 7, the model provided an accurate fit that is comparable to the fitting accuracy of SICE-3 of the flat beam. This implies that the curved beam structure is highly nonlinear compared to the previous examples.

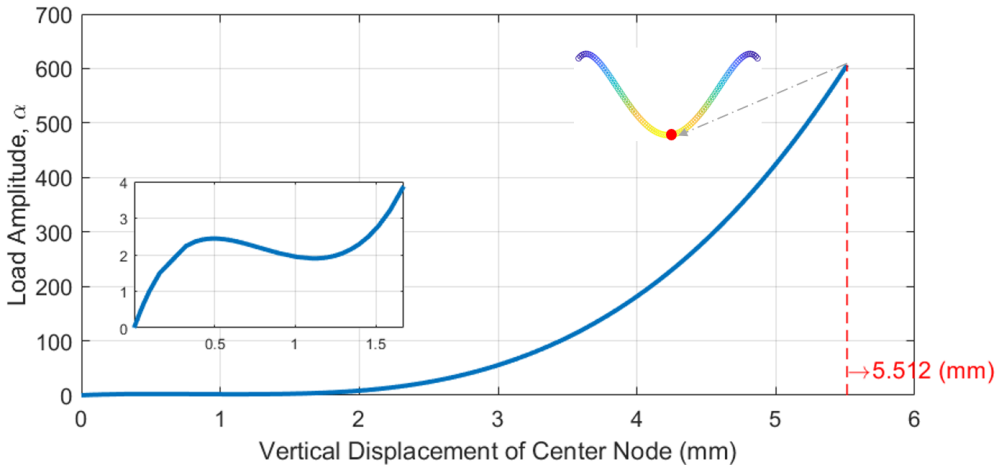

Figure 10: The quasi-static response of the curved beam for Mode 1. The curve traces the displacement of the center node of the beam model, with respect to the load scaling factor α.

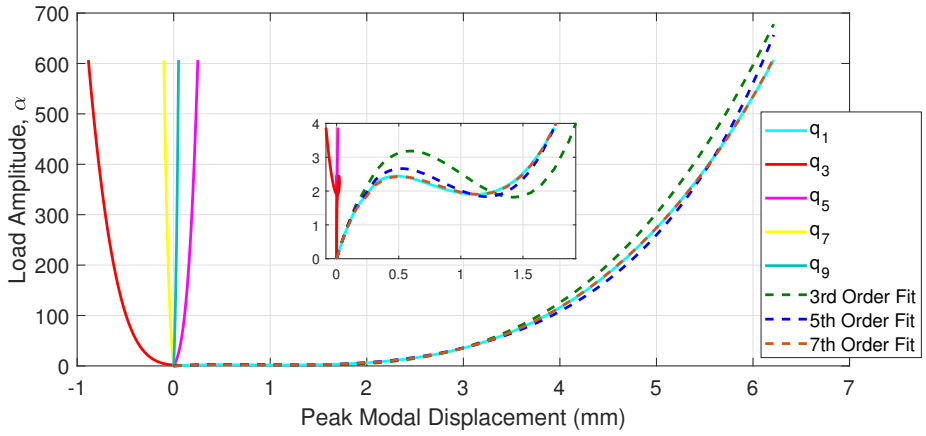

(a)

Figure 11: The quasi-static response of the first five dominant bending modes of the curved beam model. The dashed curves illustrate the least-squares fitted curves of a 3rd order, a 5th order and a 7th order SICE ROM to the first modal response curve.

Fitting order (l)	3	4	5	6	7
Fitting error (J)	3.61925	1.66701	0.42670	0.53404	0.00781

Table 5: The least-squares fit error J in Eqn. 9 to the first modal response curve of the curved beam model.

3.3.2 NNM Evaluation

The first NNM of the curved beam as computed by the secant and SICE methods are shown in Figure 12. The NNM curves were compared with a reference NNM curve that was computed with the full FE model using the MHB algorithm in [20]. Three harmonics were used to compute the backbone curve, so that some of the modal interactions could be captured. Note that an internal resonance branch appears during the softening ($q_{1,c} \approx 0.2$ mm), which will be further discussed in the Section 4. The secant method could not accurately solve for the first NNM even for the small deflections and the error significantly increased as the structure experienced the snap-through. On the other hand, the SICE-3 captured the first NNM accurately except for the snap-through region (0.2 mm $\leq x_{q,c} \leq 2.0$ mm). This is to be expected because the SICE-3 was not able to match with the snap-through region of the quasi-static response curve.

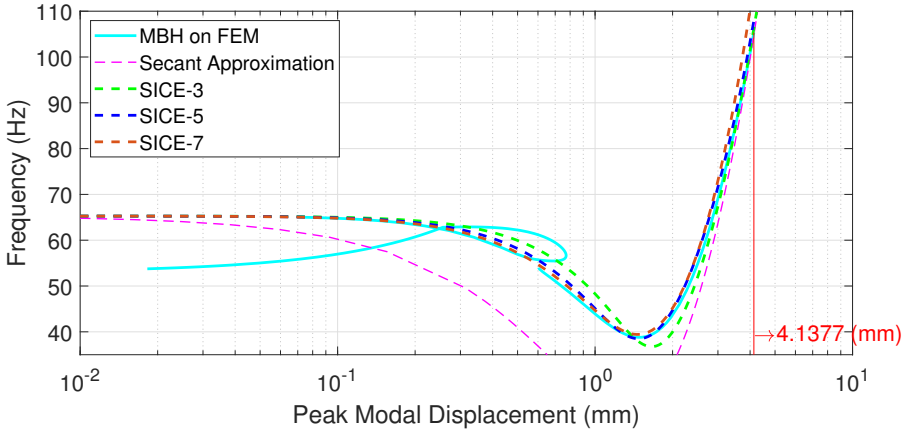

(a)

Figure 12: The first NNM curves of the curved beam in the frequency-modal response plane: the NNM curve computed by the secant method and the NNM curves computed with a 3rd order SICE-ROM (SICE-3), a 5th order SICE-ROM (SICE-5) and a 7th order SICE-ROM (SICE-7).

When the order of the SICE ROM was increased to 5, the snap-through was explained accurately as well as the hardening behavior. It is again remarkable that a SDOF model was able to accurately capture the main backbone of the first NNM of this structure, one in which modal coupling was thought to be very important [27, 37]. While the results show that the higher modes were statically coupled with the first mode, that static coupling was accurately included in the SDOF model as long as the polynomial order was high enough, and the SDOF model was able to accurately predict the backbone of the NNM. It is also important to note that the true NNM for this structure shows several important internal resonances, and those are of course not captured by the SICE model.

The SICE-7 was able to capture the NNM at snap-through a little more accurately than the SICE-5. However, it produced small errors at large deflections where the beam model experiences hardening (3.0 mm $\leq x_{q,c} \leq 4.0$ mm). We suspect that this occurs because the high order terms in the polynomial become very important at large displacements, i.e. any error in those can be significantly amplified with the order of the terms at large deflection.

4 Conclusion

This paper presented a first effort at applying quasi-static modal analysis (QSMA) to estimate the nonlinear normal modes (NNMs) of geometrically nonlinear structures. The conventional method, i.e. secant approximation, was applied to the modal response curve to compute nonlinear natural frequencies of the geometrically nonlinear FE models. The numerical results show that the NNMs of dynamic structures cannot be accurately captured by the secant method when they exhibit more complex and strong nonlinearities. Hence, we can infer that the secant method should be replaced by a more rigorous approach if QSMA is applied to bolted joints that exhibit much stronger nonlinearities. However, the results show that the basic premise of QSMA, i.e. that the nonlinear response can be inferred from quasi-static analysis, still holds even for complicated nonlinear systems. When the secant approximation was replaced with a more rigorous approach, i.e. the SICE method, the primary backbone of all of the NNMs considered was computed very accurately. SICE was found to be a reliable tool that simplifies and accelerates the NNM computation while maintaining the reasonable accuracy for the complex structures, even for the curved beam that exhibited significant modal interaction.

An advantage of utilizing the quasi-static response curve for reduced order modeling is that it reflects the nonlinearities of the structure. The quasi-static response computed by the Riks method can identify dynamically unstable regions of response as well as strongly coupled modes. Therefore, the required complexity of the reduced order model, i.e. the order of polynomial needed to explain the nonlinearities, can be guided by the quasi-static response curve. For instance, the quasi-static response of the flat beam and exhaust cover plate suggested that a 4th order polynomial was needed in order to accurately capture their monotonically hardening nonlinearities. On the other hand, the curved beam, which exhibits a combination of hardening and unstable snap-through behaviors, required a 5th order polynomial to explain the highly nonlinear response. Compared to the ICE method whose resulting ROMs are known to be sensitive to the load scaling [30], the SICE method has no need to calibrate the scaling factors of applied loads, because a sufficient number of samples distributed over the nonlinear response curve is being used for tuning the model coefficients. Furthermore, our approach provides a possibility to adaptively sample the loading cases based on the nonlinearity of the response curve, e.g. for the curved beam example, most of the samples can be chosen from the snap through response while small numbers are chosen from the stable response. It is expected that the adaptive fitting can further improve the efficiency and the accuracy of the SICE method, which is not investigated in this work and left as a future work.

The SICE ROMs that accurately fitted to the nonlinear quasi-static responses were able to accurately capture the NNMs of the FE models in all of the numerical examples considered here. Due to its compactness, i.e. a single DOF low order polynomial, it could not only dramatically reduce the computational cost but also avoid computing internal resonances of the nonlinear structures. On the other hand, the internal resonance branches cannot be filtered out when the full FE model or a multi-mode ROM is used to compute the NNMs. The curved beam example in Section 3.3.2 supports the fact that an internal resonance branch exists when the NNM was computed with the full FE model of the beam. The internal resonance branches are expensive to compute, nevertheless they are much less useful than a primary backbone curve in many NNM applications such as model validation and correlation [38]. Thus, the SICE method can be favorable when the internal resonance branches are not needed.

The proposed QSMA approach can be a useful tool for quickly estimating the NNMs of various structures. Particularly, it can be efficiently applied to model correlation and updating procedures of the nonlinear FE models that require iterative NNM computation [24–26]. In case of a SICE ROM, the number of design variables to be updated is the same as the number of nonlinear coefficients of the model, which is likely to be small, i.e. less than 4 or 5, for thin curved structures. This will accelerate computing gradients of the NNM solutions while maintaining the acceptable accuracy. Furthermore, because QSMA is based on the presumption that dynamic modal coupling is negligible (static modal coupling is preserved), it allows one to quickly assess the effect of dynamic modal coupling. In cases where dynamic coupling is found to be negligible, the analyst

or designer would be able to compute the response more efficiently and understand the dynamics using simple concepts from linear modal analysis.

Despite the effectiveness of the QSMA approach presented in this paper, there are some aspects of the approach that should be further explored. The fitting accuracy of SCIE ROM to the quasi-static response is not directly correlated to a NNM computation. The 3rd order SICE ROM of the flat beam is one example that demonstrates a small error in fitting the quasi-static response but relatively large error for the NNM solution. The sensitivity of the quasi-static response fitting with respect to the NNM solution should be further explored in a future work. Also, the proposed approach will be applied to more complex dynamic structures including highly curved beams and musical instruments such as a gong, to compare its accuracy and computational efficiency with other indirect methods.

Acknowledgments

This work was supported by the Air Force Office of Scientific Research, Award # FA9550-17-1-0009, under the Multi-Scale Structural Mechanics and Prognosis program managed by Dr. Jaimie Tiley.

References

[1] Nicos Makris and Shih-Po Chang. Effect of viscous, viscoplastic and friction damping on the response of seismic isolated structures. *Earthquake engineering & structural dynamics*, 29(1):85–107, 2000.

[2] Daniel J Segalman, Danny L Gregory, Michael J Starr, Brian R Resor, Michael D Jew, James P Lauffer, and Nicoli M Ames. Handbook on dynamics of jointed structures. *Sandia National Laboratories, Albuquerque, NM*, 871852009, 2009.

[3] EP Petrov and DJ Ewins. Analytical formulation of friction interface elements for analysis of nonlinear multi-harmonic vibrations of bladed disks. *Journal of turbomachinery*, 125(2):364–371, 2003.

[4] S Bograd, P Reuss, A Schmidt, L Gaul, and M Mayer. Modeling the dynamics of mechanical joints. *Mechanical Systems and Signal Processing*, 25(8):2801–2826, 2011.

[5] H Festjens, G Chevallier, and JL Dion. Nonlinear model order reduction of jointed structures for dynamic analysis. *Journal of Sound and Vibration*, 333(7):2100–2113, 2014.

[6] Brandon J Deaner, Matthew S Allen, Michael J Starr, Daniel J Segalman, and Hartono Sumali. Application of viscous and iwan modal damping models to experimental measurements from bolted structures. *Journal of Vibration and Acoustics*, 137(2):021012, 2015.

[7] Daniel R Roettgen and Matthew S Allen. Nonlinear characterization of a bolted, industrial structure using a modal framework. *Mechanical Systems and Signal Processing*, 84:152–170, 2017.

[8] Hugo Festjens, Gaël Chevallier, and Jean-luc Dion. A numerical tool for the design of assembled structures under dynamic loads. *International Journal of Mechanical Sciences*, 75:170–177, 2013.

[9] Hugo Festjens, Gael Chevallier, and Jean-Luc Dion. A numerical quasi-static method for the identification of frictional dissipation in bolted joints. In *ASME 2012 International Design Engineering Technical Conferences and Computers and Information in Engineering Conference*, pages 353–358. American Society of Mechanical Engineers Digital Collection, 2013.

[10] Robert M Lacayo and Matthew S Allen. Updating structural models containing nonlinear iwan joints using quasi-static modal analysis. *Mechanical Systems and Signal Processing*, 118:133–157, 2019.

[11] Gaëtan Kerschen, Maxime Peeters, Jean-Claude Golinval, and Alexander F Vakakis. Nonlinear normal modes, part i: A useful framework for the structural dynamicist. *Mechanical Systems and Signal Processing*, 23(1):170–194, 2009.

[12] Steven W Shaw and Christophe Pierre. Normal modes for non-linear vibratory systems. *Journal of sound and vibration*, 164(1):85–124, 1993.

[13] Ludovic Renson, Cyril Touzé, and Gaëtan Kerschen. Computation of damped nonlinear normal modes with internal resonances: a boundary value approach. 2014.

[14] Alexander Vakakis. Non-linear normal modes (nnms) and their applications in vibration theory: an overview. *Mechanical systems and signal processing*, 11(1):3–22, 1997.

[15] Maxime Peeters, Gaëtan Kerschen, and Jean-Claude Golinval. Dynamic testing of nonlinear vibrating structures using nonlinear normal modes. *Journal of Sound and Vibration*, 330(3):486–509, 2011.

[16] David A Ehrhardt and Matthew S Allen. Measurement of nonlinear normal modes using multi-harmonic stepped force appropriation and free decay. *Mechanical Systems and Signal Processing*, 76:612–633, 2016.

[17] Joseph D Schoneman, Matthew S Allen, and Robert J Kuether. Relationships between nonlinear normal modes and response to random inputs. *Mechanical Systems and Signal Processing*, 84:184–199, 2017.

[18] Maxime Peeters, Régis Viguié, Guillaume Sérandour, Gaëtan Kerschen, and J-C Golinval. Nonlinear normal modes, part ii: Toward a practical computation using numerical continuation techniques. *Mechanical systems and signal processing*, 23(1):195–216, 2009.

[19] Robert J Kuether and Matthew S Allen. A numerical approach to directly compute nonlinear normal modes of geometrically nonlinear finite element models. *Mechanical Systems and Signal Processing*, 46(1):1–15, 2014.

[20] Thibaut Detroux, Ludovic Renson, Luc Masset, and Gaëtan Kerschen. The harmonic balance method for bifurcation analysis of large-scale nonlinear mechanical systems. *Computer Methods in Applied Mechanics and Engineering*, 296:18–38, 2015.

[21] KD Murphy, LN Virgin, and SA Rizzi. Experimental snap-through boundaries for acoustically excited, thermally buckled plates. *Experimental Mechanics*, 36(4):312–317, 1996.

[22] Maxwell Blair, Robert A Canfield, and Ronald W Roberts. Joined-wing aeroelastic design with geometric nonlinearity. *Journal of Aircraft*, 42(4):832–848, 2005.

[23] EH Dowell. Nonlinear flutter of curved plates. *AIAA Journal*, 7(3):424–431, 1969.

[24] Simon Peter, Alexander Grundler, Pascal Reuss, Lothar Gaul, and Remco I Leine. Towards finite element model updating based on nonlinear normal modes. In *Nonlinear Dynamics, Volume 1*, pages 209–217. Springer, 2016.

[25] TL Hill, PL Green, A Cammarano, and SA Neild. Fast bayesian identification of a class of elastic weakly nonlinear systems using backbone curves. *Journal of Sound and Vibration*, 360:156–170, 2016.

[26] Mingming Song, Ludovic Renson, Jean-Philippe Noël, Babak Moaveni, and Gaetan Kerschen. Bayesian model updating of nonlinear systems using nonlinear normal modes. *Structural Control and Health Monitoring*, 25(12):e2258, 2018.

[27] Christopher I VanDamme and Matthew S Allen. Using NNMs to evaluate reduced order models of curved beam. In *Rotating Machinery, Hybrid Test Methods, Vibro-Acoustics & Laser Vibrometry, Volume 8*, pages 457–469. Springer, 2016.

[28] Marc P Mignolet, Adam Przekop, Stephen A Rizzi, and S Michael Spottswood. A review of indirect/non-intrusive reduced order modeling of nonlinear geometric structures. *Journal of Sound and Vibration*, 332(10):2437–2460, 2013.

[29] Paolo Tiso, Eelco Jansen, and Mostafa Abdalla. Reduction method for finite element nonlinear dynamic analysis of shells. *AIAA journal*, 49(10):2295–2304, 2011.

[30] Robert J Kuether, Brandon J Deaner, Joseph J Hollkamp, and Matthew S Allen. Evaluation of geometrically nonlinear reduced-order models with nonlinear normal modes. *AIAA Journal*, 53(11):3273–3285, 2015.

[31] T. L. Hill, V.R. Melanathuru, and S. A. Neild. Capturing nonlinear modal coupling and interactions in reduced-order models. *7th International Conference on Nonlinear Vibrations, Localization and Energy Transfer*, 2019.

[32] E Riks. An incremental approach to the solution of snapping and buckling problems. *International journal of solids and structures*, 15(7):529–551, 1979.

[33] RW Gordon, JJ Hollkamp, and SM Spottswood. Nonlinear response of a clamped-clamped beam to random base excitation. In *Proceedings of the Eighth International Conference on Recent Advances in Structural Dynamics*. The Inst. of Sound and Vibration Southampton, England, UK, 2003.

[34] Joseph J Hollkamp, Robert W Gordon, and S Michael Spottswood. Nonlinear modal models for sonic fatigue response prediction: a comparison of methods. *Journal of Sound and Vibration*, 284(3-5):1145–1163, 2005.

[35] David A Ehrhardt, Matthew S Allen, Timothy J Beberniss, and Simon A Neild. Finite element model calibration of a nonlinear perforated plate. *Journal of Sound and Vibration*, 392:280–294, 2017.

[36] Adam Przekop and Stephen A Rizzi. Nonlinear reduced order random response analysis of structures with shallow curvature. *AIAA journal*, 44(8):1767–1778, 2006.

[37] Christopher I VanDamme and Matthew S Allen. Nonlinear normal modes of a curved beam and its response to random loading. In *Nonlinear Dynamics, Volume 1*, pages 115–126. Springer, 2017.

[38] Chris I VanDamme, Matthew Allen, and Joseph J Hollkamp. Nonlinear structural model updating based upon nonlinear normal modes. In *2018 AIAA/ASCE/AHS/ASC Structures, Structural Dynamics, and Materials Conference*, page 0185, 2018.